



## Review on WO<sub>3</sub> Thin Films: Materials Properties, Preparation Techniques and Electrochromic Devices

M.Jayachandran<sup>1\*</sup>, R.Vijayalakshmi<sup>3</sup>, Visalakshi Ravindran<sup>2</sup> and C.Sanjeviraja<sup>4</sup>

<sup>1</sup>ECMS Division, Central Electrochemical Research Institute, Karaikudi 630 006, TN, India

<sup>2</sup>EMFT Division, Central Electrochemical Research Institute, Karaikudi 630 006, TN, India

<sup>3</sup>Department of Physics, Thiagarajar College, Madurai 625 009, TN, India

<sup>4</sup>Department of Physics, Alagappa university, Karaikudi 630 003, TN, India

Received: 25 December 2004 Accepted: 3 March 2005

### Abstract

With recent advances in engineering, thin film technology is playing an increasingly important role in spearheading technological advancement of future society. Aside from traditional applications, thin film technology is also closely tied to nanotechnology, which is one of the key technologies of the near future. Thin films play a dominant role in modern technology like optoelectronics, microelectronics, etc. Generally thin films have thickness between 0.1 μm and 30 μm and must be chemically stable, well adherent, well to the surface, uniform, pure, and have low density of imperfections. There are a number of different techniques that facilitate the deposition of stable thin films of oxide materials on a silicon wafer and on other suitable substrates of conducting or insulators. Common materials include silicon dioxide, tin oxide and transition metal oxides. Electrochromic materials, especially transition metal oxides like WO<sub>3</sub> and MoO<sub>3</sub>, are able to change their optical properties in a reversible and persistent way under the application of a voltage pulse. These materials are currently of interest for displays, rear-view mirrors and smart windows for energy saving. Because WO<sub>3</sub> is the best suited material for energy conservation application, materials properties before and after colouration and its electrochromic mechanism are elaborately given in this review. The enormous flexibility provided by thin film growth technique allows the fabrication of desired geometrical, topographical, physical, crystallographic and metallurgical structures in two or lesser dimensions. These features are increasingly being exploited to tailor make the structure sensitive physical, mechanical, chemical and electrochemical properties of micro materials. All the techniques used to prepare WO<sub>3</sub> thin films are summarised with an elaborative account on the electrodeposition technique along with our results.

### Introduction

Electrochromics is a field of science and technology mainly driven by the technological goal of being able to turn a transparent glazing into a color tinted glazing and then turn it back again. The subject is inter-disciplinary. It is electrochemistry, and mostly involves actively modifying electrodes in an electrochemical cell in which positive ions are discharged at one electrode and created at the other. It is solid state physics since the discharged positive ions, guest atoms,

are free to diffuse in a thin solid film of host material (quite essentially WO<sub>3</sub>) modifying its electronic structure to create colored material in some very important cases. Further more the questions of structure, phase change, surface distortion, grain boundary effects, crystalline Vs amorphous, amongst many other related topics, arise. It is chemistry when sol gel deposition methods are used. It is vacuum science and technology when sputter deposition or evaporation is used to make thin films of suitable host material. It is polymer science when organic / polymers are used. It is electronics in control methods. For all its promise the field of electrochromic

\* Corresponding author: M.Jayachandran

E-mail address: jayam54@yahoo.com

systems has only become successfully commercialized in one area, namely mirror systems for cars: this is based on redox reactions in solution involving substances as Wurster Blue. In spite of its commercial success this is very much an area for a wide range of systems and presents a challenge to our understanding of their redox operation and the accompanying physicochemical and structural changes.

Electrochromism has been known for several decades as far as the first statement made in 1953. Tungsten trioxide was one of the first transparent metal oxides (Table 1) whose electrochromism was studied and reported. Thin films of  $WO_3$  and other oxides have been deposited in a number of ways to develop electrodes with electrochromic properties.

Table 1. Cathodic and anodic electrochromic materials

Cathodically ion insertion materials	Anodically ion insertion materials	Color of oxidized state	Colour of reduced state
$MoO_3$		Transparent	Blue
$V_2O_5$		Yellow	Blue-Black
$Nb_2O_5$		Yellow	Blue
$WO_3$		Transparent	Blue
	$In(OH)_3$	Blue Black	Transparent
	$Ni(OH)_2$	Brown-bronze	Transparent / green

### Crystal structure of $WO_3$

Tungsten oxide or the tungsten trioxide has perovskite like atomic configurations based on corner sharing  $WO_6$  octahedra (Fig. 1a). The crystal structure has been studied by high resolution microscopy, and the extended defects are characterized by crystallographic shear planes, pentagonal bipyramidal columns, and hexagonal and pentagonal cross-sections. Fig. 1b shows the three dimensional structure of  $WO_3$ .

Deviations from the ideal cubic perovskite like structure correspond to antiferroelectric displacements of W atoms and to mutual rotations of oxygen octahedra. Tungsten oxide has a tendency to form substoichiometric phases containing edge-sharing octahedra. The overall compositions can be expressed as  $WO_{3-z}$  with  $Z > 0$ . Most of the structures can be viewed as magneli phases of the series  $W_mO_{3m-1}$  and  $W_mO_{3m-2}$  ( $m=1,2$ ). The structure of the types  $W_{26}O_{77}$  ( $Z=0.04$ ),  $W_{20}O_{58}$  ( $Z=0.1$ ),  $W_{40}O_{116}$  ( $Z=0.17$ ),  $W_{18}O_{49}$  ( $Z=0.28$ ) and others are also possible. The properties of W are given in Table 2(a) and the coordinates of W and O in  $WO_3$  lattice are shown in Table 2(b). The structural, electrical and optical properties of  $WO_3$  are summarised in Table 3.

Table 2(a). Properties of tungsten in the  $WO_3$  lattice

Name	Tungsten
Symbol	W
Atomic number	74
Group	Transition metal
Density at 293K	19.3g/cm <sup>3</sup>
atomic weight	183.85
Ionization energy	770KJ/M
Electronegativity	2.36
Melting point	3683.2K
Boiling point	5773K
Heat of vaporization	824.0KJ/M
Heat of fusion	35.40KJ/M

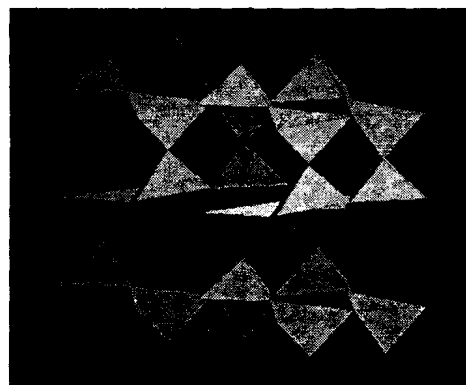


Fig. 1a. Corner-sharing arrangement of octahedra in  $WO_3$  lattice

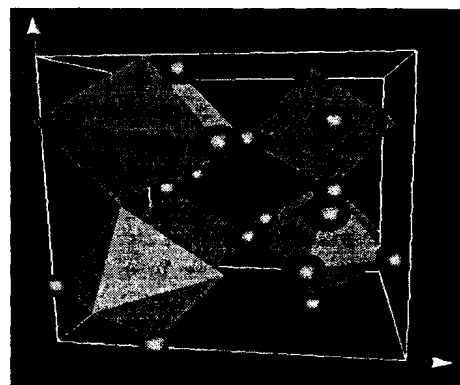


Fig. 1b. Three dimensional structure of  $WO_3$  crystal

Table 2(b). Coordinates of W and O

Atom	x	y	z
W	0.256	0.229	0.053
O(1)	0.25	0.03	0.00
O(2)	0.00	0.25	0.00
O(3)	0.25	0.28	0.50

Table 3. Structural, electrical and optical properties of WO<sub>3</sub> film

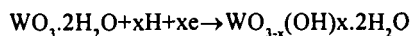
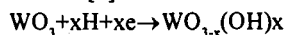
Crystal	Monoclinic, Hexagonal
Semiconductor type	n type
Molecular weight	231.84
Carrier concentration	$2 \times 10^{20} \text{ cm}^{-3}$
Indirect band gap	2.70 – 3.25 eV
Refractive index	2.5
Bulk density	7.169 g/cm <sup>3</sup>
Melting point	1472°C
Electrical conductivity	$2 - 4 \times 10^4 \Omega^{-1} \text{ cm}^{-1}$
Absorption coefficient	$10^4 \text{ cm}^{-1}$
Dielectric constant	20.2
Electrochromic property	(i) Fresh - colourless (ii) Colored – Blue (iii) Bleached – colour less
Coloration efficiency	Li <sup>+</sup> ~ 50-75 cm <sup>2</sup> /columb K <sup>+</sup> ~ 20 to 50 cm <sup>2</sup> /columb H <sup>+</sup> ~ 30 to 40 cm <sup>2</sup> /columb

### Structural Studies of WO<sub>3</sub> Films

In tungsten trioxide, the magnitude of the distortion depends on the temperature, which is in agreement with the behaviour of most perovskites, and pure WO<sub>3</sub> single crystals, go through structural transformations according to the sequence tetragonal→orthorhombic→triclinic→monoclinic, as the temperature is lowered from 900 to -189° C. TsumotoTsao and Akira Kishimoto [1] reported that various tungstates with a defective hexagonal or pyrochlore-type framework, which are built out of six membered rings or corner sharing WO<sub>6</sub> octahedra, can be obtained by thermal decomposition of an amorphous salt precipitation by reacting peroxy tungstic acid with a solution of alkaline halide. As these compounds are synthesized in oxidizing atmosphere, they are fully oxidized tungstates such as potassium tungsten bronze (hexagonal) and their framework may be lacunar. Kudo et al [2] reported the crystallographic data of xBaO.WO<sub>3</sub> produced at 530°C and xCs<sub>2</sub>O.WO<sub>3</sub> formed at 500° C and indexed in the hexagonal system except for weak peaks due to the impurity upper temperature phases. Hydrates WO<sub>3</sub>.1/3H<sub>2</sub>O have been obtained by hydrothermal treatment of an aqueous suspension of either tungstic acid gel, or crystallized dehydrate for the first bronze. The complete structure arises from the stacking of such layers along the [001] direction, every other layer being shifted by a/2 and the structural water is localized in O(4) and bonded to W(2). The dehydration led to the metastable phase hexagonal WO<sub>3</sub> [3]. Tungsten oxides exist in several polyforms and it has received much attention because of its three dimensional channel structure, the octahedral represent the WO<sub>6</sub> building blocks and mobile

cations, such as Li, H, Na, and K can be inserted into the vacant channel of the structure. The x-ray diffraction patterns of the film showed many diffraction peaks which can be mainly divided into two kinds of tungsten oxides, one with a hexagonal tungsten bronze structure and the other with pyrochlore structure [4].

The X-ray diffraction patterns of the as-deposited and annealed oxides are reported for the sintered tungsten trioxide film electrode [5]. Before and after cathodic polarization at -0.3V for coloration, the pattern was assigned based on the cell constants of WO<sub>3</sub> with monoclinic (pseudo orthorhombic symmetry with a=7.303Å, b=7.54Å, c=7.692Å and β=90.881°). Even after the polarization at -0.3V for 0.5h, no change was observed on the XRD pattern in spite of the fact that the electrode had been already colored blue. Meanwhile, several XRD pattern assigned to the orthorhombic hydrogen bronze H<sub>x</sub>WO<sub>3</sub>(x=0.1) started to appear after a polarization for two hours at the same potential. After 12 hours the WO<sub>3</sub> film completely transformed to the bronze phase. It is reported that there are four kinds of hydrogen tungsten bronzes, i.e. monoclinic for x < 0.02, orthorhombic for x ≈ 0.1, tetragonal for 0.15 ≤ x ≤ 0.23 and cubic for x > 0.23. No hydrogen bronze other than the orthorhombic one was observed in the XRD patterns of the sintered WO<sub>3</sub> film electrodes even by further polarization up to -1.0V<sub>SCE</sub>. The XRD patterns are reported for an anodic electrode prepared from sputtered tungsten film on the tantalum substrate in 0.5M H<sub>2</sub>SO<sub>4</sub> at 293 K. XRD measurements on electrocoloration of WO<sub>3</sub> electrodes is attributed to the formation of hydroxyl type hydrogen bronze. It is also found that the electrochromic property in WO<sub>3</sub>.2H<sub>2</sub>O is independent of the structure; this indicates that the electrocoloration is not due to the formation of oxygen vacancy. The possibility two types of electrocoloration processes are considered possible for the film electrodes of WO<sub>3</sub> and WO<sub>3</sub>.2H<sub>2</sub>O as follows [5]:



The XRD pattern of the tungsten film deposited at 773°K is analyzed. The peaks corresponding to metallic tungsten of the WO<sub>3</sub> phase also has the metallic properties for the films prepared with silicon substrate. It has been shown that the electrical resistance of sub-stoichiometric WO<sub>3</sub> CVD films deposited by W(CO)<sub>6</sub> pyrolysis and activated with gold mono layers presents reversible changes in the presence of hydrogen while it remains unaffected by the presence of the O<sub>2</sub>, SiO<sub>2</sub> and propanol vapours [6]. Reichman and Bard [7] reported that the pair of peaks at 2.64 and 2.66 Å<sup>0</sup> is due to the

characteristic property of the triclinic structure. Schutcher *et al.*, [8] reported that XRD spectra of  $WO_3$  thin film material have the triclinic characteristic peaks at  $2\theta=27.14^\circ$  and  $44.87^\circ$ .

Scalfani *et al.*, [9] reported that the peak at  $2\theta=39.9^\circ$  is attributable to bare  $WO_3$  with the triclinic structure by the catalysis preparation. Maruyama and Arai [10] reported that the d values for (222) and (002) plane which appeared in the spectrum, indicated that the film is composed of crystallites with triclinic structure for the chemical vapour deposition at  $400^\circ C$ . The diffraction of the intrinsic film shows that it is stoichiometric triclinic  $WO_3$ , reported by Yu *et al.*, [11]. Hutchins *et al.*, [12] reported that the peak at  $2\theta=30^\circ$  is due to the  $WO_3$ .

From d values, Machido and Enyo [13] explained that the electrocolouration of  $WO_3$  is attributed to the formation of hydroxyl type hydrogen bronze and also the electrochromic property in  $WO_3 \cdot 2H_2O$  is independent of the structure of the films produced by RF sputtering method. This indicates that the electrocolouration is not due to the formation of oxygen vacancy. Patil [14] reported that the  $WO_3$  films deposited at various substrates temperatures showed different structures and was clearly observed that below  $350^\circ C$  the films are amorphous. The presence of (020) diffraction peak indicates the gradual long range atomic order developments above  $350^\circ C$ . The changes in the structures are particularly large when the substrate temperatures are between  $400^\circ$  and  $450^\circ C$ . This suggests that the crystal structure of tungsten oxide is susceptible to the deposition temperature. As substrate temperature increases, the film goes through structure transformations as monoclinic-triclinic-hexagonal-tetragonal. Ngygen Van Nha *et al* [15] reported that the structural properties of tungsten oxide films deposited on glass substrates by evaporating  $WO_3$  powder in a vacuum of about  $10^{-5}$  torr. Glass substrates were degreased in organic solvents and rinsed in de-ionized water. The deposited film without annealing shows amorphous phase and after annealing at a temperature of  $300^\circ$  for 2 hours the film transformed into the crystalline phase. The film exists not only in the  $WO_3$  phase but also in undesired phases, such as  $W_{25}O_{73}$  and  $W_{18}O_{49}$ . It reveals the characteristic XRD pattern with triple peaks and the diffraction peaks at (220) and (202) are also observed. As-deposited tungsten oxide films did not show any peaks when subjected to x-ray diffraction but when substrates were subjected to post heat treatment at  $400^\circ C$  for 10 minutes duration diffraction peaks for (021) and (001) planes of a monoclinic  $WO_3$  [16] were observed. When the tungsten trioxide films were colored by the electrolytes containing hydrogen ions,

the crystal structure is changed due to the induction of the hydrogen ions into  $WO_3$  interstitial sites. The new peaks at  $2\theta=23.85^\circ$  and  $33.55^\circ$  could be assigned to the characteristic peaks of hydrogen tungsten bronze with tetragonal structure parameters  $a=3.751\text{ \AA}$ ,  $c=3.79\text{ \AA}$  in bleached state. The diffraction pattern reversed almost entirely similar to the initially colored state. When Li ions are inserted, two peaks at  $2\theta=23.6^\circ$  and  $33.6^\circ$  were assigned to cubic lattice constant of the (100) and (110) planes and (200) and (220) planes of  $WO_3$  disappeared. But in the bleached state the diffraction peak are returned [17]. Dae-Sik Lee *et al* [18] reported that the XRD patterns of the tungsten trioxide thin film deposited by thermal evaporation method, annealed at  $600^\circ C$  for two hours showed triclinic structure. Also they revealed that the different substrates did not create any great change in the structure and grain size of the tungsten trioxide thin films. Fang *et al.*, [19] obtained the triclinic structure for the  $WO_3$  films prepared by the pulsed laser ablation technique.

Vijayalakshmi *et al* [20,21] have reported triclinic structure for their electrodeposited  $WO_3$  films as shown in Fig.2 and d-values with index for the as-deposited and reduced films are given in Table 4.

Table 4. Comparison of d values with JCPDS for the as-deposited and reduced  $WO_3$  films

Experimental		JCPDS	(h k l)
As-deposited	reduced		
3.3738	3.3722	3.36	1 2 0
2.7993	2.7988	2.714	0 2 2
2.6634	2.6612	2.667	2 0 2
2.0649	-----	2.08	2 0 3

High grade metal tungsten (Merck) powder of high purity and hydrogen peroxide solution are used for electrodeposition by Vijayalakshmi *et al.*, [20]. Triple distilled water free from impurities, was used to prepare the required mole concentration of the electrolyte. The various deposition parameters of  $WO_3$  are optimized (Table 5) for getting stoichiometric films, which are well-adherent, uniform and pinhole free with a deep blue color.

Table 5. Optimized parameters for the  $WO_3$  electrodeposition

Parameter	Value
Galvanostatic current density	0.5 mA/cm <sup>2</sup>
pH	2
Bath temperature	300K
Concentration	0.1N
Deposition time	90 minutes
Substrate	FTO

**Structure of intercalated WO<sub>3</sub> Films**

The diffraction pattern of the WO<sub>3</sub> film shows that it is stoichiometric triclinic WO<sub>3</sub> while the intercalated film (the film in the intercalated state) shows the hexagonal structure, and the deintercalated film once again shows the triclinic structure. Tables 6 and 7 show the variation of 'd' values for various H<sub>2</sub>SO<sub>4</sub> concentration and for the ion intercalated/deintercalated films respectively and the values are compared with the JCPDS values. Fig.3a, b, c shows the X-ray diffractograms of the as-deposited, and reduced state of WO<sub>3</sub> films in 0.1, 0.5, 1.0N H<sub>2</sub>SO<sub>4</sub> respectively. [Vijayalakshmi *et al* [21,22,23].

Table 6. Comparison of d values with JCPDS for ion introduction in H<sub>2</sub>SO<sub>4</sub>.

Experimental as-deposited	d (Å)			JCPDS	(hkl)
	0.1 N	0.5 N	1.0 N		
3.300	3.339	3.364	3.365	3.320	(1 2 0)
2.744	2.793	2.793	2.656	2.714	(0 2 2)
2.612	2.656	2.655	-	2.640	(2 2 0)
2.039	2.062	2.062	-	2.080	(2 0 3)

Table 7. Comparison of d values with JCPDS for ion intercalation in HNO<sub>3</sub>

Intercalated	JCPDS	(h k l)	deintercalated	JCPDS	(h k l)
3.12	3.165	2 0 0	3.36	3.36	1 2 0
3.12	3.165	2 0 0	2.794	2.714	0 2 2
2.65	2.66	1 1 1	2.653	2.667	2 0 2
2.381	2.388	2 1 0	2.015	2.011	2 1 3
1.77	1.75	3 1 0	1.77	1.71	2 0 4
1.68	1.65	2 0 2	1.685	1.69	0 2 4

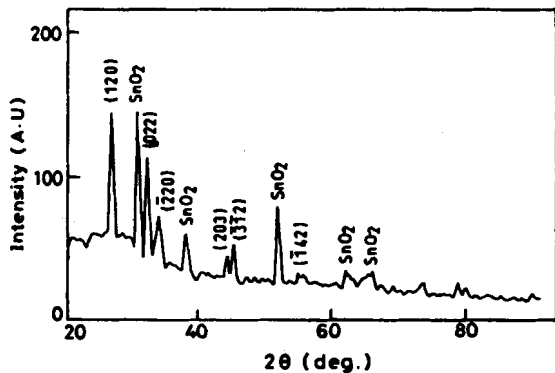


Fig.2. XRD pattern of galvanostatically deposited WO<sub>3</sub> film

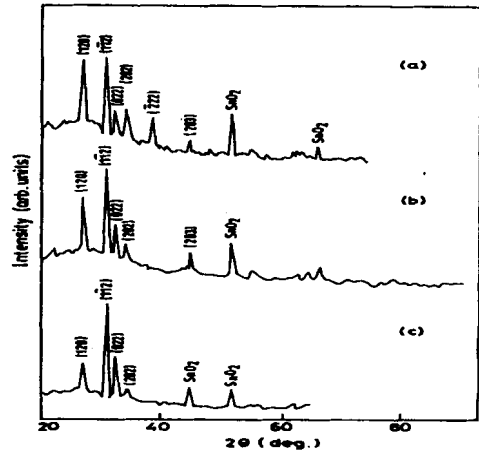


Fig.3. XRD pattern of WO<sub>3</sub> films reduced in a) 0.1N b) 0.5 N and c) 1.0N H<sub>2</sub>SO<sub>4</sub>

**Structure of Ni doped WO<sub>3</sub> films**

The as-deposited WO<sub>3</sub> and the Ni doped WO<sub>3</sub> films were uniform and well-adherent to the substrates so that they could withstand many times of coloring/bleaching cycles without any deterioration. From the growth kinetics, the deposition rate of the Ni-doped films was found slightly larger than the un-doped films. The incorporation of additional metals into thin tungsten oxide film has a marked effect on the color of both the freshly prepared neutral oxide and the bronze (Ni+W) oxide formed by the electrodeposition method. Fig.4a and b show the diffraction pattern of the electrodeposited WO<sub>3</sub> and Ni doped WO<sub>3</sub> films respectively [24].

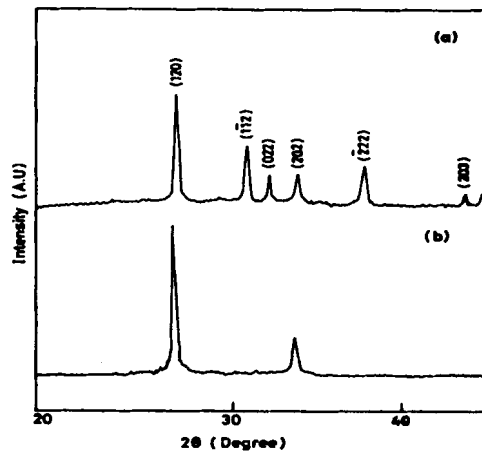


Fig.4. XRD pattern of a) as-prepared and b) Ni-doped WO<sub>3</sub> film

The diffraction pattern of  $WO_3$  films shows that it has stoichiometric triclinic structure while the doped films were with considerably different peak patterns in which the Bragg peaks are slightly shifted to lower side, but retaining the peak intensity similarly high. Table 8 gives the comparison of the inter-planar distance (d) of these two samples with the JCPDS values. Yu *et al* [11] reported that the doped  $WO_3$  film prepared on the nickel substrate had different XRD peaks compared to the films deposited on ITO substrates.  $WO_3$  and nickel doped  $WO_3$  films are successfully prepared by the simple electrodeposition method. The structural properties are studied by XRD and it shows triclinic structure for both the  $WO_3$  and nickel doped films. But the XRD pattern for doped film showed different peak heights when compared to that for undoped  $WO_3$  film.

Table 8. XRD data of  $WO_3$  with doping of nickel

Sl.No	Observed for $WO_3$	d(A) JCPDS	hkl	Ni doped $WO_3$
1	3.373	3.320	(120)	(120)
2	2.925	3.070	(112)	---
3	2.799	2.714	(022)	(022)
4	2.663	2.632	(202)	---
5	2.380	2.202	(222)	---

### Crystal structure of tungsten bronzes

Tungsten bronzes can be represented as  $M_xWO_3$  with M being an atom from the first column in the periodic table as shown in Fig.5. They can be prepared in bulk with crystalline nature from vapour-phase reactions. Tetragonal phases are found at low and intermediate x values for  $Li_xWO_3$ ,  $K_xWO_3$  and for high  $Na_xWO_3$  respectively. The phase domains are shifted towards smaller x values at elevated temperature [25,26].

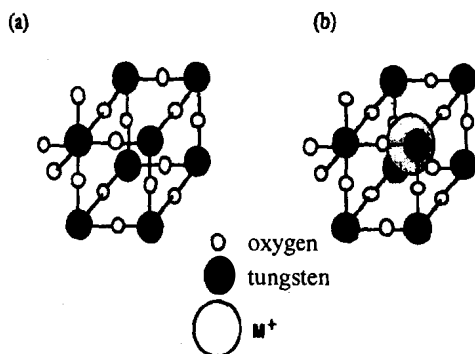


Fig.5. Crystall lattice of (a)  $WO_3$  and (b) the perovskite bronze product of reduction,  $M_xWO_3$ .

The occurrence of hexagonal phases for small incorporation of large ions in  $K_xWO_3$ ,  $Cs_xWO_3$  systems are of considerable interest for electrochromics, which were analyzed by Magneli [27]. A pyrochlore structure can be stabilized in Rb and Cs tungstates [28-32]. It can serve as a host for intercalation of  $Li^+$  and other possible ions [33-36].

The hydrogen ions are thought to be statistically attached to the oxygens as hydroxyl groups, so the material may adequately represented as  $WO_3(OH)_x$  [37].

### Preparation techniques

#### Evaporation technique

Tungsten oxide was deposited by thermal evaporation of  $WO_3$  powder from the molybdenum boat on various substrates which increased the temperature during evaporation from room temperature up to about  $150^\circ C$ . The  $WO_3$  thin films for IR measurement were prepared by the vacuum evaporation of monoclinic tungsten oxide on silicon plates. Palladium catalyst was deposited on the  $WO_3$  film by subsequent vacuum evaporation [38].

#### Electrodeposition technique

The anode was platinum foil and cathode was ITO glass plate. The cathodic electrodeposition was performed at a current density of  $200 \mu A/cm^2$  in 0.5 M of  $Na_2WO_4$  aqueous solution (pH=7) at room temperature. The films were uniform, adhesive and transparent. The solution was prepared by dissolving powdered tungsten metal in 20 ml of hydrogen peroxide. When the reaction was completed, excess peroxide was decomposed by dipping a platinum electrode into solution until the effervescence ceased [39,40].

Electrodeposition of thin film depends on a variety of parameters viz. galvanostatic current, pH and concentration of the electrolyte, bath temperature, deposition time and the type of the substrate [20, 21]. 2 g of pure tungsten (Merck) powder was mixed with 20% solution of hydrogen peroxide giving high temperature at the same time effervescence is produced. Few drops of  $H_2SO_4$  was slowly added until the effervescence ceased completely. Transparent conducting F-doped tin oxide (FTO) coated glass substrate having about  $10 \Omega/cm^2$  sheet resistance was used as cathode for galvanostatic deposition. A platinum foil as counter electrode and a standard calomel electrode as the reference electrode were used. Deposition was carried out using EG&G PAR 362 potentiostat at a current density of  $0.5 mA/cm^2$ . Growth kinetics were studied with thickness versus time of deposition. As the time is increased, the thickness of the film is increased linearly

upto 90 minutes. After this time, the thickness remains constant and reaches saturation which is termed as terminal thickness and the films started peeling-off above this thickness.

Deposition of  $WO_3$  films containing a second metal ion (as dopant) can be easily prepared by electrochemical technique, by just adding a metal chloride salt solution ( $NiCl_2$ ) solution of 0.2 M into the readily prepared electrolyte with  $W+H_2O_2$  in the ratio of 1:1. The films were deposited galvanostatically at the optimized current density of  $0.5mA/cm^2$  and the bath temperature was kept constant at  $30^\circ C$ . Brownish colored films were obtained by Vijayalakshmi *et al* [24] and the films were of uniform thickness (0.2 to  $0.4 \mu m$ ).

### Spray pyrolysis technique

Spraying of aqueous solutions of metatungstic acid ( $H_6W_{12}O_{39}$ ) was reported by Hurditch [41] and Zeller and Beyeler [42]. Spray deposition, using solutions of  $WCl_6$  dissolved in ethonal or NN-dimethyl formamide, was carried out [43—46] where spraying took place in air on to substrates heated upto  $500^\circ C$ . The W oxide films thus formed showed electrochromic property. XPS data gave evidence of some Cl contamination in the film. XRD showed that films deposited at temperatures more than  $300^\circ C$  were crystalline. Sivakumar *et al* [47, 48] have deposited monoclinic  $WO_3$  films at  $250^\circ C$  and the electrochromic properties are reported.

### Electron beam evaporation technique

The standard technique for making W oxide films suitable for laboratory studies was the condensation of a vapor produced by sublimation from hot  $WO_3$  powder. The heating can be produced by a resistive boat (Ta, Mo and W) or by a refraction crucible or by an electron beam. Water free powder is sometimes used. The substrate can be unheated or kept at a temperature up to a few hundred degrees, and the evaporation can take place under non-reactive gas. The evaporation technique is well known for yielding films with good electrochromism and is widely used for thin films made by electron beam evaporation. This technique can increase the deposition rate at the expense of having a smaller surface which is evenly coated, simply by placing the substrate closer to the vapour source. The vapour produced by heating  $WO_3$  does not consist of individual atoms but is molecular in nature. The dominating species is trimeric  $W_3O_9$  molecules, dependent on experimental conditions [49]. The deposition rate was 4-5 ( $\text{Å/s}$ ), the deposition angle was varied within  $40^\circ$  with a planetary rotation, and the substrate temperature was usually maintained at  $80^\circ C$  after keeping at  $110^\circ$  for 5 min. The total

gas pressure in the chamber during the evaporation process was controlled by  $N_2$  gas introduction and maintained to be  $5.0 - 6.5 \times 10^{-2}$  Pa. Deposited  $WO_3$  films were analysed by electron diffraction and found to be amorphous. The packing density of the film, calculated from the film thickness and weight, was  $5.38g/cm^3$  [50]. Sivakumar *et al* [51] have studied the optoelectronic properties of  $WO_3$  films electron beam evaporated at different substrate temperatures.

### Sputter deposition technique

Thin film formation by sputtering usually involves the bombardment of a target material with accelerated ions, the evaporation of target material and its deposition on a substrate. If a reactive species such as oxygen or methane is present in the gas phase, a chemical reaction with the evaporated target material can occur, leading to the deposition of a chemical compound. In the past, reactive sputter deposition processes were widely used for the preparation of oxides, carbides, nitrides, silicides or oxy-nitrides. The surface and volume microstructure of the deposited compounds depend strongly on the preparation procedure. Sputter deposition is a well established technique for industrial thin film preparation. Sputter deposited W oxide films cannot be expected to exhibit the same composition and micro structures as in films made by evaporation of  $WO_3$ . The reason is that the deposition process involves the dislodging of species from a target by ion impact at energies large enough for breaking up molecular  $WO_3$  bonds when sputtering is carried out from an oxide target or from an oxidized metal target. Tungsten oxide films were deposited on substrates by means of reactive DC-magnetron sputtering, like quartz, Cr coated glass and transparent conducting glass ( $In_2O_3:Sn R_{sq} = 10 \text{ ohm/sq}$ ) and were used for transmittance, Raman scattering and electrochemical measurements [52].

The tungsten oxide films were produced by reactive DC-magnetron sputtering from a 5.1 cm diameter metallic tungsten target. The target electrode was set in the bottom side of the chamber and was water cooled. Substrates for deposition were Indium tin oxide (ITO) coated glass ( $15 \text{ ohm/sq}$ ) which were heated to  $400^\circ C$ . The chamber was initially evacuated to less than  $2 \times 10^{-5}$  torr. Oxygen/argon mixtures were used as the sputter ambient. The total pressure of the mixture was 70 millitorr with 15%  $O_2$ .

### RF sputtering

The data for DC and RF sputtering are given Kaneko *et al* [53] and Akram *et al* [54] respectively. Beyond a certain  $O_2$

content, the rate goes down and approached a constant value of 0.1 nm/s. This decrease is due to oxidation of the sputter target. An analysis of the sputter discharge parameters for W oxide preparation can be found in [55] and higher sputter rates can be accomplished by increasing the powder density of the target. The highest rate is 3.4 nm/s, which was reported by Hichwa *et al* [56] for reactive magnetron. By selecting appropriate sputter parameters, one can avoid stress build up in the deposited films [57] and increase the porosity by oblique angle sputtering [58]. Tungsten oxide thin films were deposited by RF sputtering from a  $WO_3$  target (12 cm in diameter). The sputtering atmosphere was an Ar-10% oxygen mixture in a total gas pressure of 5 millitorr. The RF power was 200 W operated at 13.56 MHz. Ultrasonically cleaned alumina and glass slides, over coated with a 5 nm layer of amorphous carbon, were used as substrates. The substrates were mounted on a holder and maintained at a constant temperature of 300° C. The target was pre sputtered for 30min and the main sputtering was performed [59]. Polycrystalline sample of  $WO_3$  was prepared by RF sputtering on to a substrate held at  $325 \pm 10^\circ C$  in an atmosphere of 10% oxygen and 90% argon at 40 millitorr. The characterization of the structure was determined by X- ray diffraction measurements. A bath of 1N  $H_2SO_4$  with 10% glycerol (by volume) was used as the ion source/electron insulator for coloration and bleaching of the  $WO_3$  layer. The results of the spectroscopic ellipsometry measurements of the optical constants for the polycrystalline  $WO_3$  (in various status of coloration) are independent of reflectivity measurements [60].

### Sol-gel technique

Sol-gel derived films can be made from colloidal solutions by dipping, spin-coating or spraying. The colloidal oxide can be obtained through a poly condensation process either by acidification of an aqueous salt or by hydrolysis of an organo-metallic compound. The sol-gel technique has been surveyed [61-66] in the most widely studied technique, used by Chemseddine *et al* [67-71] and others [72-76]. Acidification was accomplished by pursuing a solution based on  $Na_2WO_3$  or  $K_2WO_4$  through a proton exchange resin. The ensuing solution, which underwent spontaneous polymerization, was applied to glass plated either directly as drops or by spin coating and spraying. After drying by heating, it was possible to obtain hard coatings with good electrochromism and some optical isotropy. W-PTA sols were prepared in 18 ml of (30%)  $H_2SO_4$  which reacted with small percentage of metallic powder [5g, 91%]. The mixture was stirred for 12 hours at

room temperature until the tungsten powder had dissolved. A Platinum net was then added to the mixture to remove any unreacted  $H_2O_2$ . The sols with a deep brown color were stored at  $-25^\circ C$  to prevent gellation prior to dipping. This gellation process can be reversed by adding small amount of  $H_2O_2$  until the dark brown sol is reformed [77]. Films were obtained by heat treatment. The thickness of the fresh films were in the range of 150nm/dipping upto 5 dippings and were performed yielding 600 nm thick films [78]. Dip coating using a solution of tungsten hexaethoxide or tungsten oxo-tetra butoxide has been applied successfully, by Bell *et al* [79] and others [80] respectively. A substrate was dipped into this solution and after a meniscus had settled, the substrate was withdrawn at a constant rate of the order of 10 nm/s. The layer was dried at room temperature for 1 hour to vapourize the solvent.

### Surface morphology by SEM/AFM studies

The SEM photograph of the pulsed electrodeposited  $WO_3$  thin film has smooth surface as reported by Zhenuri *et al.*, [11]. Scalfani *et al.*, [9] reported small platelets (crystals) for the tungsten trioxide thin films deposited on the  $SnO_2$  surface. No big change of crystal size on tungsten trioxide thin films was reported by Fang *et al* [19]. The results of the SEM surface morphology of the chemical vapor deposited  $WO_3$  films for various concentrations were reported [80]. According to Shen Tesung [81], it is advantageous to have an alcohol addition to form good thin films. To have the optimized electrochromic properties, annealing treatment is preferred. An all solid state electrochromic device employing prussian blue and electrodeposited tungsten trioxide thin film with polyethylene oxide gel electrolyte was fabricated by Su *et al* [80]. Fig.6 shows the surface morphology of  $WO_3$  film prepared by spray pyrolysis technique [47].

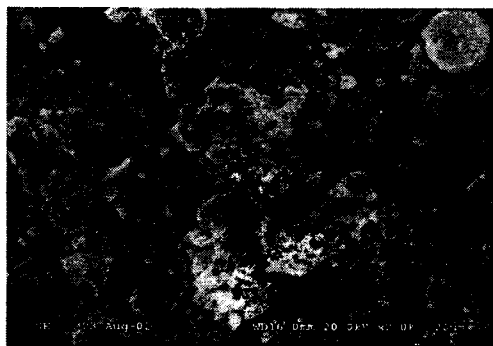


Fig.6. SEM picture of  $WO_3$  film prepared by spray pyrolysis technique

Highly uniform surface morphology was observed for the  $WO_3$  films with spherical particles deposited by electron beam evaporation technique on TCO substrates at  $200^\circ\text{C}$  as shown in Fig.7 [51]. Fig.8a and b shows the SEM picture of the as-electrodeposited  $WO_3$  films and the surface after  $H^+$  ion intercalation respectively by Vijayalakshmi et al [23]. AFM morphology of  $H^+$  ion intercalated  $WO_3$  film is also shown in Fig.9. Fig.10 shows the AFM picture of Ni doped  $WO_3$  film prepared by electrochemical technique [24].

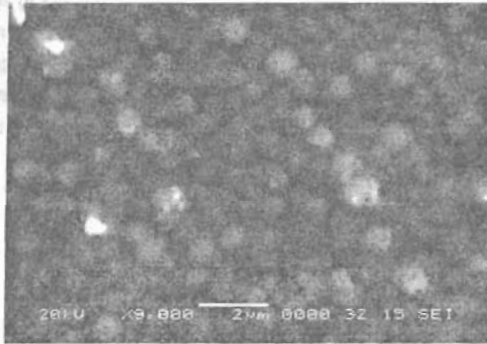


Fig.7. SEM morphology of  $WO_3$  film deposited by electron beam evaporate technique

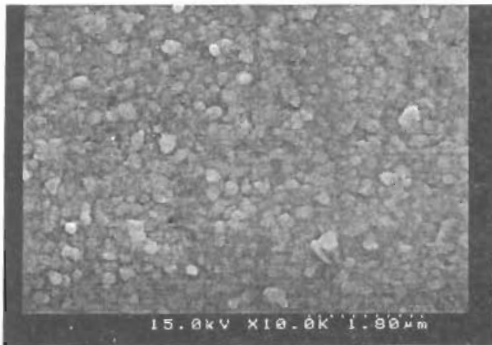


Fig.8 a. SEM picture of electrodeposited  $WO_3$  film

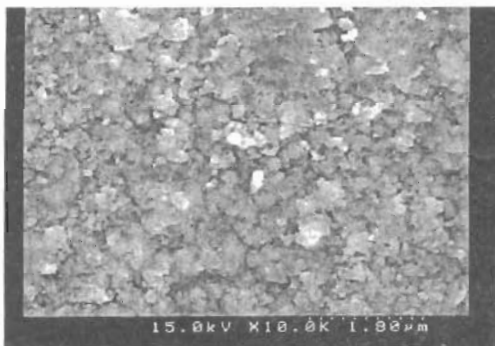


Fig.8 b. SEM picture of  $WO_3$  film after  $H^+$  ion intercalation

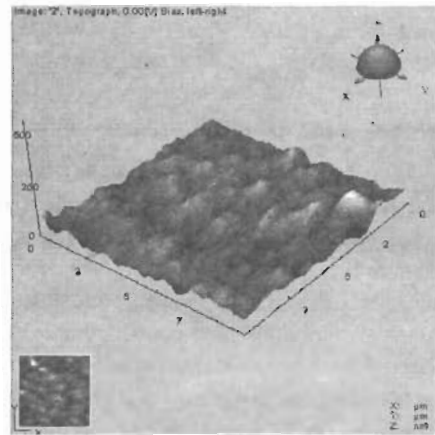


Fig.9. AFM picture of electrodeposited and  $H^+$  ion intercalated  $WO_3$  films

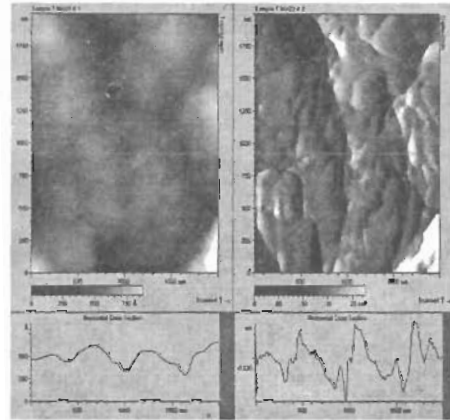


Fig.10. AFM picture of Ni doped  $WO_3$  film by electro deposition

### Impedance Analysis

Complex plane analysis of evaporated  $WO_3$  films on conducting tin oxide (CTO) coated glass substrate has been performed in propylene carbonate electrolytes as a function of frequency from 100kHz to 100MHz at various applied voltages. It has been confirmed that the electron injection process at the CTO/ $WO_3$  film interface, the electrochemical charge transfer process in the  $WO_3$  and the diffusion controlled process in the bulk are the important processes at high ( $f > 1\text{kHz}$ ), medium ( $1\text{kHz} < f < 3\text{Hz}$ ) and low ( $f < 3\text{Hz}$ ) frequencies respectively. The change of electrochromic activity at various  $WO_3(H_2O)$  films depends mainly on the charge transfer process in the film. The charge transfer

impedance increases with hydroxylation of the  $\text{WO}_3$  layer and, further more, increases drastically with hydrated crystallization [82, 83].

### Ion intercalation and deintercalation

Reversible color bleach (CB) cycles can be attained using the tungsten trioxide films as the working electrode. According to the double injection mode, some amount of protons (and electrons) can be extracted during the first bleaching procedure. By repeating the CB cycles of injected protons introduced during coloration period becomes equal to that of extracted protons during subsequent bleaching periods [84]. The extent of coloring/bleaching and in particular the speed of bleaching the (the coloring is not affected by the speed) to a larger extent depends on film thickness [85]. Cyclic voltammograms of tungsten trioxide films were measured in propylene carbonate (PC) electrolyte [86]. The cathodic current is associated with the bleaching process of the film and the anodic current is associated with the coloring process of the film. It was about +360 mV/s Vs SCE for the as-deposited film and for the film stored in  $\text{LiClO}_4$ -PC electrolyte for 20 hours at 70°C it was +50 mV Vs SCE. The shift continued gradually with storage time after the initial drastic shift. These cathodic shifts result in the decrease of the injection charge in the coloring on reaction, which was contributed to the degradation of electrochromic activity of the  $\text{WO}_3$  film. With respect to the anodic oxidation of the colored  $\text{WO}_3$  film, the anodic reaction becomes fast with the storage of the film [87]. Fig. 11 shows the cyclic voltammetric behaviour of the electrodeposited  $\text{WO}_3$  films in different concentrations of  $\text{H}_2\text{SO}_4$  to study the intercalation/deintercalation property [20]. Fig. 12 shows the cyclic curves obtained in 0.1N  $\text{H}_2\text{SO}_4$  at various scan rates [21]. The  $\text{WO}_3$  film obtained by vacuum evaporation method, a typical current-potential (I-V) curve of the  $\text{WO}_3$  film electrode in 1M  $\text{H}_2\text{SO}_4$  was reported [88]. Lianyoung su *et al* [89] explained that the film exhibited reversible photochromic and electrochromic behaviour of blue coloration with absorption in the near IR region. Ohtsuka *et al* [90] explained that the oxide film has been formed anodically on tungsten electrode at a potential of 1.0V (Vs RHE) in 0.1 mol  $\text{dm}^{-3}$  sulphuric acid and perchloric acid solutions. The compositions and electrochromic behaviour of the films have been examined by in-situ ellipsometry and Raman spectroscopy. The electrochromic coloring of the film takes place at a potential lower than that of 0.5V and light absorption increases with decreasing potential, where it is directly proportional to the amount of cathodic charge passed during

the colouring process. The electrochromic reaction is initiated by electron transfer from the metal substrate and proton transfer from the aqueous acidic solution to the oxide. Electrochemical properties of evaporated amorphous  $\text{WO}_3$  films on conductive glass substrates have been studied by Nobyeki Yoshiike *et al* [91]. In order to classify the influence of water on electrochromism stored in high humidity atmosphere, films prepared by vacuum evaporation have been studied in organic electrolytes [92-94]. Nilgun Ozer *et al* [93] and Unuma *et al* [95] discussed the developments in sol-gel deposited electrochromic film. Tungsten oxide is the common semiconducting film used in solid state electrochromic devices, prepared from a number of sol-gel precursors such as tungsten acid solutions [96] and tungsten alkoxides based solutions [97, 98].

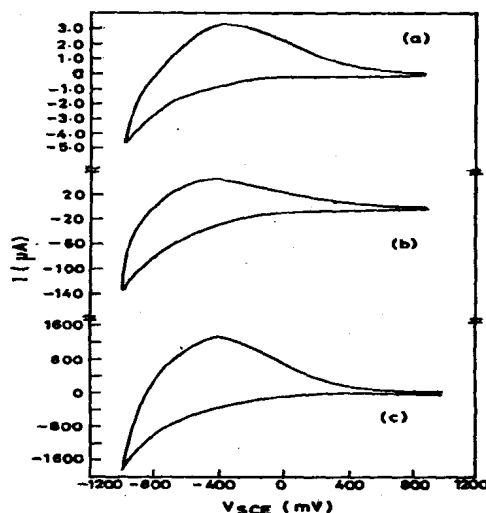


Fig.11. I-V curves of  $\text{WO}_3$  film in a) 1.0 N b) 0.5 N and c) 0.1 N  $\text{H}_2\text{SO}_4$

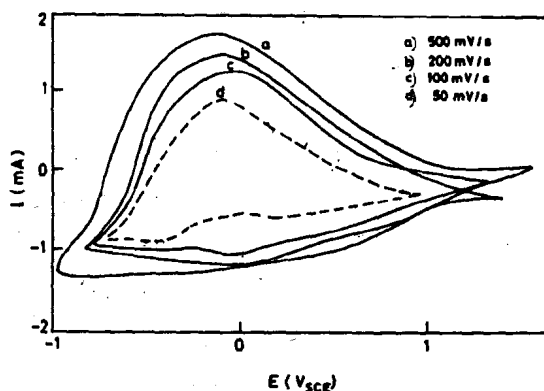


Fig.12. I-V curves of  $\text{WO}_3$  in 0.1  $\text{H}_2\text{SO}_4$  at different scan rates

Films prepared from chloro-alkoxide showed better uniformity than those prepared from colloidal route. Preparation of Tungsten oxide, vanadium and nickel hydroxide and polymeric substrates covered with indium tin oxide thin film were discussed [98]. A detailed study of H<sup>+</sup> ion intercalation into the electrodeposited WO<sub>3</sub> films were reported by Vijayalakshmi et al [22]. The diffusion coefficient values of H<sup>+</sup> ions of different concentration, during anodic and cathodic scan, are given in Table 9 [20-24].

Table 9. Parameters associated with intercalation and deintercalation of H<sup>+</sup> ions

Concentration	Anodic peak Current I <sub>pa</sub> (μA)	Cathodic peak Current, I <sub>pc</sub> (μA)	Diffusion Co-efficient for I <sub>pa</sub> 10 <sup>-11</sup> cm <sup>2</sup> /S	Diffusion Co-efficient for I <sub>pc</sub> 10 <sup>-11</sup> cm <sup>2</sup> /S
1N	1400	1900	2.69	3.10
0.5N	3.20	4.20	0.98	2.08
0.1N	0.35	1.40	1.35	2.70

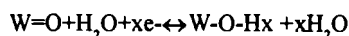
### Infrared and Raman spectroscopy

IR absorption spectroscopy is a powerful technique particularly for elucidating changes in hydration and hydroxylation that occur upon ion intercalation/deintercalation. Despite the obvious merits of this technique, and the general availability of IR spectrophotometers, it has been employed in the limited number of studies, and that data obtained are not consistent. This feature is almost certainly due to different compositions of the films. However, this technique of vibrational spectroscopy gives information that is complementary to the one from the Raman spectra. The fundamental reason is that infrared active modes are related to dipole moments whereas Raman active modes are related to the polarizability tensor. The IR data can provide clear evidence on the hydrogen-oxygen framework. The infrared spectra for as-deposited and annealed in air at 260°C for one hour films was reported. A pronounced H-O-H deformation band at 1602 cm<sup>-1</sup> was observed in the infrared spectrum of the as-deposited film. This is due to the structural water coordinated as H<sub>2</sub>O molecules. A broad band at 3518 cm<sup>-1</sup> corresponds to the O-H stretching vibration. When the film was heated at 260°C, the absorption peaks at 1602 cm<sup>-1</sup> and 3518 cm<sup>-1</sup> almost vanished [98]. A detailed study of solutions used for sol-gel deposition with tungsten chloro alkoxide precursors was given by Judenstein et al [98-102]. Raman spectra have been reported by Nanbe et al [103] and Nonaka et al [104] which shows that the as-deposited film has a strong peak at

about 960 cm<sup>-1</sup> which is assigned to stretching vibrations of terminal W=O bonds and a broad peak centered at 660 cm<sup>-1</sup>. The spectrum is similar to the one for anodic oxide films prepared at a low voltage, and the peaks at 660 cm<sup>-1</sup> can be explained analogously for the two types of samples. It remains as a possibility that the sol-gel material should be regarded as composed of iso poly tungstate species [105]. After treatment at 109°C for 2 hours in air, the peak at 960 cm<sup>-1</sup> decreased in strength and strong feature developed around 700 cm<sup>-1</sup>. IR absorption results of thin W oxide films made by sputtering of WO<sub>3</sub> along with O<sub>2</sub> and Ar+O<sub>2</sub> vapours was reported by Akram et al [106] and Daniel et al [107]. Absorption due to H-O-H deformation was found at 1600 cm<sup>-1</sup> and due to O-H stretching at 3400 cm<sup>-1</sup> which shows that these sputter deposited WO<sub>3</sub> films were hydrous. Aging in air studied by Daniel et al [107] led to a noticeable increase in the water absorption band due to W-O remained unchanged. After several days, new absorption peak appeared at 1425 cm<sup>-1</sup> corresponding to W-O-H deformation, and the O-H stretching band split into three components centered at 3440 cm<sup>-1</sup>, 3220 cm<sup>-1</sup> and 3050 cm<sup>-1</sup>. Nobyeki Yoshiike et al [91] studied evaporated W oxide films immersed in LiClO<sub>4</sub> and a broad band around 800 cm<sup>-1</sup> was observed due to the tungsten-oxide framework. The absorption due to various O-H stretching modes at about 3400 cm<sup>-1</sup> and weak absorption due to H-O-H deformation modes in molecular water at about 1600 cm<sup>-1</sup> were observed. Storing the film in 0.3 M lithium perchlorate at 70 °C - 260 °C for 500 hours within a closed container yielded the spectrum represented by solid curves and the O-H stretching was more intense. The changes in the low frequency modes may indicate some modification in tungsten oxygen framework. The powders of H<sub>2</sub>WO<sub>4</sub> and Li<sub>2</sub>WO<sub>4</sub>, which was taken as an indication of Li and replacing the hydrogen ion on inner surfaces of the films [100]. For evaporated W oxide films, which were intercalated and deintercalated as well as in electrolytes containing sodium and potassium ions. The most salient feature is the increase of the O-H stretching mode intensity at 3400 cm<sup>-1</sup> which occurs in direct correspondence with the quantity of inserted charge and correlation was verified with the heights of the absorption peaks and areas under such peaks. The amount of molecular water, on the other hand, was found to be low irrespective of the charge insertion. Here the phenomenological model involves the following processes: alkali ions replacing protons on the pore surfaces, insertion of the liberated protons in interstitial position in the tungsten trioxide lattice, and adsorption of the water molecule next to the W=O bond. But Pickelmann and

Schlottter [108] reported that the spectrum was rather unaffected by the process and the absorption at  $3400\text{ cm}^{-1}$  did not change much, which was taken as evidence that the intercalated protons did not bind the bronsted sites at the pore surfaces. Badilescu *et al* [109] showed that intercalation with hydrogen from  $\text{H}_2\text{SO}_4$  was associated with the development of broad absorption band around  $1170\text{ cm}^{-1}$  and a narrow band at  $1030\text{ cm}^{-1}$  and shoulders at  $930$  and  $870\text{ cm}^{-1}$ . The process of intercalation/deintercalation in  $1\text{N H}_2\text{SO}_4$  was studied for the sputter deposited W oxide films by Yamada *et al* [110]. Without inserted charge the same absorption features appear as in the IR spectra. Charge insertion leads to the evolution of an intense broad absorption band and increase of a band centered at  $2400\text{ cm}^{-1}$  in proportion with the charge, and simultaneous smaller decrease of a band at  $3400\text{ cm}^{-1}$  and  $2400\text{ cm}^{-1}$  band was referred to the hydroxyl groups in the  $\text{WO}_3$  matrix. Daniel *et al* [107] reported that the absorption spectra has at  $1620\text{ cm}^{-1}$  for proton intercalation and occurrence of a narrow absorption band at  $950\text{ cm}^{-1}$ . The former band was assigned to water presumably in protonated form. Spin coated W oxide films produced from a solution of

$\text{WCl}_6$  in 2-propanol, were found to have  $3400\text{ cm}^{-1}$  and  $1600\text{ cm}^{-1}$  bands which was consistent with intercalation of  $\text{H}^+$  and or  $\text{H}_2\text{O}$ - due to  $\text{W}=\text{O}$  and  $\text{W}-\text{O}$  bonds by the following reactions:



Oral *et al* [84] reported that the peaks having the same value for  $\text{WO}_3$  film by the sol-gel method. Reichman and Bard [7] reported the IR spectra of  $\text{WO}_3$  film prepared by the thermal evaporation method showing a broad peak at  $1650$  and  $3500\text{ cm}^{-1}$  which is the characteristic property peaks of water. FT-IR spectrum of the  $\text{WO}_3$  film deposited by the electron beam evaporation method reported by Nobyeki Yoshiike *et al* [88] on a Si wafer stored in  $0.3\text{M LiBF}_4$ -PC electrolyte in a sealed glass tube at  $70^\circ\text{C}$ , the shoulder of O-H stretching broad peak at  $3400\text{ cm}^{-1}$  was decreased as same as in  $\text{LiClO}_4$ -PC electrolyte while W-O stretching broad peak at  $650\text{ cm}^{-1}$  was rarely changed. A detailed FTIR analysis was carried out for the electrodeposited  $\text{WO}_3$  films [22, 23]. Fig.13 shows the FTIR spectra of the  $\text{WO}_3$  films after  $\text{H}^+$  ion intercalation. The vibrational modes and their assigned frequencies for the  $\text{WO}_3$  films, before intercalation and after intercalation are given in Table 10.

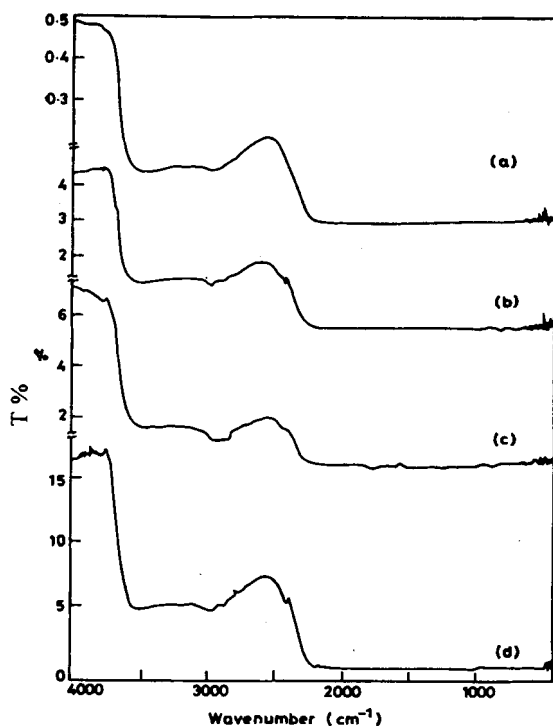


Fig. 13. FTIR spectra of  $\text{WO}_3$  films a) before intercalation and after intercalation

Table 10. FTIR values of  $\text{WO}_3$  films before and after intercalation

Before intercalation			
Wave Number	Band Assignment		
674.963	W-O-W Corner Sharing		
724.139	W-O-W Edge Sharing		
855.275	W-O-W		
2200.380	Hydroxyl Bond		
3543.560	OH-H		
3758.580	Coloration		
After Intercalation			
	0.5 N	0.1 N	1.0 N
Band Assignment			
838.88	835.00	814.770	W-O-W
2358.52	2377.800	2364.300	Hydroxyl
3564.77	3564.770	3731.580	OH-H
3737.37	3749.000	3749.900	Coloration

The Raman Spectrum of the  $\text{WO}_3$  films obtained by electrodeposition route is show in Fig.14 [24]. The peaks observed at  $705\text{ cm}^{-1}$  and  $803\text{ cm}^{-1}$  are clearly indicating the monoclinic structure for this electrodeposited  $\text{WO}_3$  film.

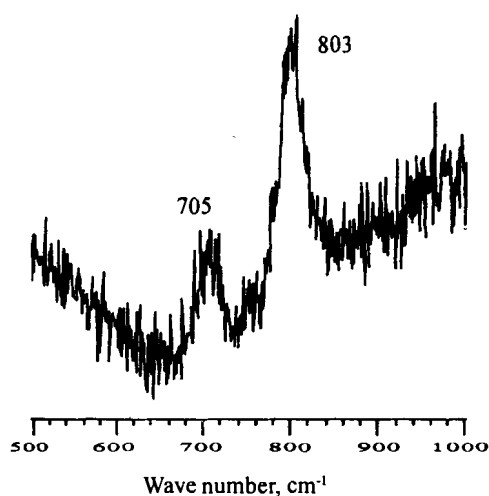


Fig.14. Raman spectrum of electrodeposited  $\text{WO}_3$  film

### Optical properties

Development of semiconducting oxide materials with controllable energy gap is necessary for the increased applications in electrochromic liquid crystal display and optoelectronic devices. Hence the absorption and transmission properties were studied in detail to calculate the band gap variations and the related optical properties. For heavily disordered evaporated  $\text{WO}_3$  films band gap varied from 3.2 to 3.4 eV [111-121]. The band gap depends on the materials preparation conditions and was diminished in films evaporated onto substrates at elevated temperature. Miyake *et al* [122] reported a monotonic drop of  $E_g$  with increasing temperature. The band gap was changed from 3.25 eV to 2.7 eV. The decrease is strongest at temperature  $>300^\circ\text{C}$  which indicates that crystallization is causing the band gap narrowing for sputter deposition, the band gaps have been reported  $3.0 < E_g < 3.4$  eV [111,123-126]. For sputter deposition the authors reported 3.0 to 3.4 eV with a tendency that a high pressure of the sputter gas and high  $\text{O}_2$  admixture in reactive sputtering. This process gave a low  $E_g$  [127-131]. Crystallized films made by sputtering had  $E_g = 2.9$  eV [132-133] and by chemical vapour deposition showed a bandgap 3.2 eV [134-135]. A thickness dependent change in the crystallinity or W oxide films made by anodizing, results have been reported that 3.05 and 3.73 eV [136-140]. Crystalline anodic films with monoclinic triclinic, and orthorhombic structure and different degrees of hydration had the band gap of  $2.55 < E_g < 2.79$  eV as seen from the photo electro-chemical measurements [138,141-142]. Takaya Kubo and Yoshinori Nishikitani [143] reported that the optical band gap converges to a constant value between

2.8 and 2.7 eV assigned to crystalline  $\text{WO}_3$  film. The hydrogen tungsten bronze is a reasonable semiconductor at low values of  $x$  of  $\text{H}_x\text{WO}_3$  [143-145] varying from the above ratio.

Von Rottkay *et al* [146] recorded the optical measurements with a variable angle spectroscopic ellipsometer from 280 to 1700 nm. Upon coloration the agreement between effective medium theory and optical measurements deteriorates. The injected electrons are trapped at the energetically lower sites, thus giving the compound the character of the preferred component, possibly the one with smaller atomic number. Films prepared in the sol-gel process showed the good transmission modulation at wavelength higher than 520 nm, more than 50% and at lower wavelength the transmittance was very less [147]. All transmittance and reflectance spectra showed the typical interference structure caused by both ITO and  $\text{WO}_3$  layers. Absorbance of tungsten trioxide increases with injected charge but also with increasing wavelength creating the typical blue colour of the tungsten bronzes. The incomplete oxidation of evaporated tungsten oxide does not lead to the expected optical absorbance [148]. Azens *et al* [149] reported that the transmittance for an as-deposited film increases strongly as one goes towards longer wavelengths in the luminous range. This feature was not typical for electrochromic W oxide films. At the same time the luminous transmittance of unpolarized light is 46% at  $+60^\circ$  and 35% at  $-60^\circ$  in the as-deposited state whereas the corresponding numbers are 15% and 9% in the coloured state. This clearly manifested that angular selectivity may be of interest for applications of electrochromic smart windows, inclined windows, glass blinds and louvers.

The reflectance spectra of  $\text{WO}_3$  films showed significant reflectance variation in the infrared region which coincides to sputtering deposited  $\text{WO}_3$  film [150, 151]. Golden and Steele [152] reported that in the normal transmission mode, the electrochemically lithiated  $\text{WO}_3$  films showed brown colouration on high levels of lithiation. The transmission spectra for  $x=0.3$  and 0.5 show a very broad peak in the near IR regions. Bader *et al* [153] reported a theoretical outline for the reflection and transmission spectra obtained from spectroscopic ellipsometer technique on thin films deposited on a thick transparent substrate. The optical parameters are shown as a function of the wavelength for the as deposited  $\text{WO}_3$  film before insertion of lithium.

The observed optical variation in the tungsten trioxide films are comparable to the reported results for the tungsten trioxide films prepared by electrochemical [154] and thermal evaporation [155] techniques. In the potassium ion

intercalation process, the transmission spectra of the  $\text{WO}_3$  film deposited on TCO exhibits an extremely high degree of transmission (80%) in the as-deposited state. After intercalation, there is a sudden fall in the transmittance spectra, but after deintercalation, the transmittance is recovered but it is slightly less than that for the as-deposited film. Fig.15 shows the transmittance spectra of the electrodeposited  $\text{WO}_3$  films before intercalation [22, 23]. After intercalation, there is a reduced transmission behaviour in the studied spectral region which became higher after deintercalation as shown in Fig. 16 a and b respectively. The transmission is quite low for the sputtered tungsten trioxide dispersed in PMMA. However, charge extraction was quite slow, or charge injection was partially irreversible [157]. The absorption spectra alone do not allow to distinguish between the polaron and free-carrier absorption but it was unlikely that free-carrier absorption appeared in the as-deposited films with an essentially amorphous structure. Oral et al [155] explained that the  $\text{WO}_3$  films, deposited using a dip coating method from peroxy poly tungstic acid sols, exhibit good gasochromic properties reflected by large colouring/bleaching changes and good kinetics.

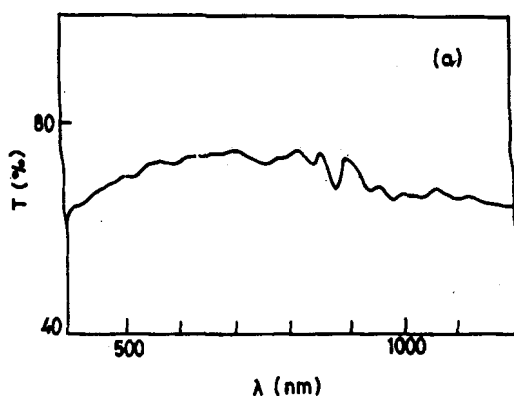


Fig.15. Transmission spectrum of electrodeposited  $\text{WO}_3$  film

However the gasochromic colouration was still inferior to that observed for electrochemically coloured films prepared without catalyst. The gasochromic response and speed of the coloring/bleaching kinetics were improved by increasing molar ratio of palladium and tungsten from 1:25 to 1:40. In order to establish the difference between the vibrational properties of bleached/coloured films, the vibrational parameters were explained by applying the classical model [159].

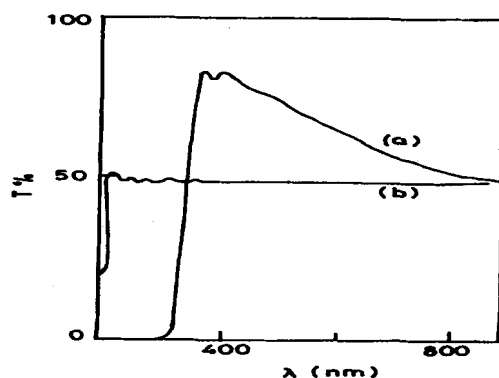


Fig.16. Transmission spectrum of  $\text{WO}_3$  film a) before and b) after intercalation

### Electrochromic devices using $\text{WO}_3$ film

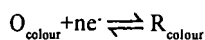
In general there are only two types of electrochromic devices. In the first type, the electrodes are made of conducting glass and covered with an organic or inorganic polymer. These materials usually display complementary electrochromism and produce the same color change when one is oxidized and the other is reduced. This type of configuration was used in electrochromic windows and is bistable. It means that once the color change has occurred, the state of the device remains even in the absence of applied voltage. The limitation of this type of electrochromic devices is its slow color change due to the low migration rate of the counter ions in the bulk polymer. Bright color changes are not possible here.

In the second type, two complementary electrochromic molecules are dissolved in a solvent. It is very simple to build, reacts very fast and can produce dark or bright colors. The drawback is that an electrical current is needed to maintain the colored state. The colored molecules diffuse through the system and react to restore the bleached states. It cannot be used for large area devices.

To overcome these problems an electrochromic system is needed which is both bistable and changes color rapidly. The above processes can be accomplished by attaching a suitable molecule that is colorless in the oxidized state and colored in the reduced state onto the surface of a colorless semiconducting electrochromic material (present case,  $\text{WO}_3$ ) on conducting glass FTO substrates. When a sufficiently negative potential is applied, electrons are injected from the conducting glass into the conduction band of the semiconducting electrochromic material and reduce the absorbed molecules. The reverse process occurs when a positive potential is applied and the molecules get bleached. The advantage of this system is that

it combines immobility of the electrochromic material with the rapidity and coloration efficiency of the molecular systems. The ultimate interest in the electrochromic materials is the fabrication of electrochromic device, which can control the transmittance or the reflectance of the incident light. The practical applications of electrochromic device include the smart window, information display, rear-view mirror in the automobile, protection glassware etc. The principles of these devices are explained briefly in this section.

Tungsten oxide was the first discovered material with clear-cut electrochromism and is the most viable option for electrochromism based devices. The crystal structure is of perovskite-type, but some atomic displacement and rotations of  $\text{WO}_6$  octahedra normally occur so that, depending on the temperature, tetragonal, monoclinic, or triclinic symmetries are formed. A generalized form of the electrochromic reaction may be written as



where an electrode acts as the source or sink of electron(s). During the electrochromic reaction of thin film metal oxides, the electrons responsible for the colour center or leave the oxide film via the interface with the electrode while the ions necessary for charge balance (electro neutrality) enter or leave the film via the ion conductive electrolyte. A species is said to be electroactive if it can undergo electron uptake (reduction) or electron release (oxidation) type reactions at an electrode. Electroactive species have different numbers of electron in their oxidized and reduced forms, so each redox state has different electronic (UV-Vis) spectra owing to different absorption bands. The difference in optical properties, on electron transfer, is detected by the eye as a different colour for each redox state. In cases, where changes in spectra are quite marked, the concept of a useful color change has been advanced such that electrochromism can be defined as 'the electrochemical generation of colour in accompaniment with an electron transfer reaction [160]. There are four main applications needed of electrochromic devices and are shown in Fig.17.

1. *Information display:* This device embodies an electrochromic film in front of a diffusely scattering pigmented surface. A seven segment numeric display unit of small or large size is the best example (Fig.17 a).
2. *Mirror with variable specular reflectance:* This application seems to be the most mature and application oriented one. Anti dazzling rear-view mirrors built on electrochromic oxide films are now-a-days used in cars and trucks (Fig 17 b).

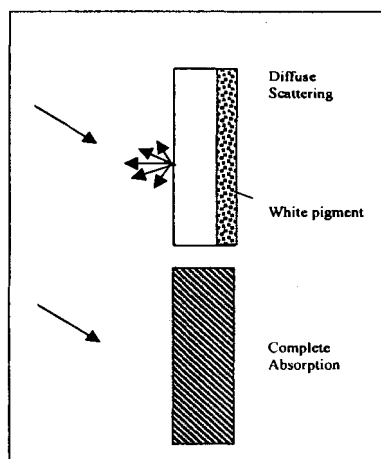


Fig.17(a) Information Display device

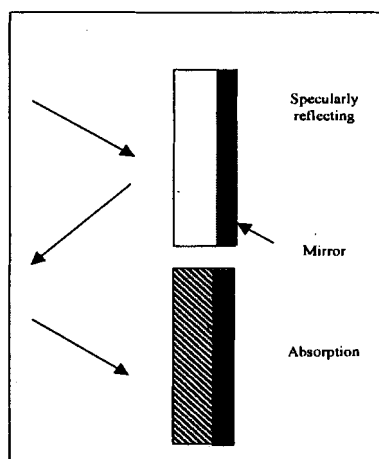


Fig.17(b) Variable Reflectance Mirror

3. *Smart windows:* The basic idea is to develop an automotive window with variable transmittance so that a desired amount of visible light or solar energy is permitted in a controlled manner (Fig. 17 c) introduced. Such windows can lead to energy savings as well as a comfortable and cool indoor climate.
4. *Variable emittance surfaces:* This is based on a special device design with a crystalline tungsten oxide film at the exposed surface of an electrochromic device (Fig. 17 d). Intercalation/deintercalation of ions makes this surface infrared reflecting or absorbing whose thermal emittance from the high.

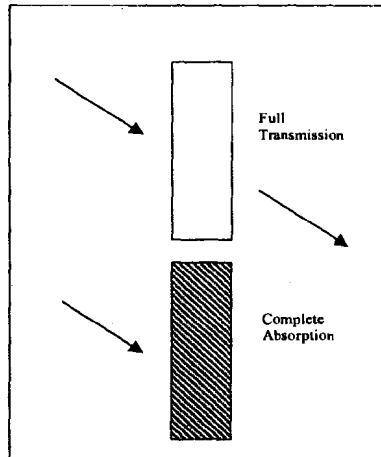


Fig.17(c). Smart Window

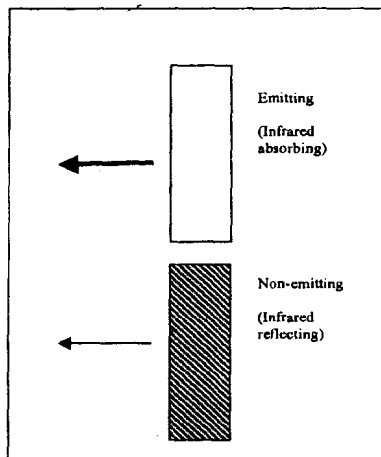


Fig.17(d). Variable Emittance Surface

### Conclusion

Devices based on electrochromism with their tunable transmission for visible and infrared radiation will play an important role for architectural and automotive glazing. As  $\text{WO}_3$  is thermodynamically stable at room temperature, it is considered as the most suitable material for the electrochromically active electrodes in the electrochromic devices. The materials properties, preparation techniques, colouration/bleaching efficiency and the electrochromic devices developed are elaborately presented in this review.

### References

1. Tsumoto Tsao and Akira Kishimoto, *Solid State Ionics*, 59 (1993) 211

2. T.Kudo, A.Kishimoto and J.Oi, *Solid State Ionics*, 40/41 (1990) 567
3. B.Gerand and L.Seguin, *Solid State Ionics*, 84 (1996) 199
4. A.Yu, *Solid State Ionics*, 100 (1997) 267
5. Ken-ichi Machida and Michio Enyo, *J. Electrochem. Soc.*, 137 (1990) 1169
6. Takaya Kubo and Yoshinori Nishikitani, *J. Electrochem. Soc.*, 145 (1998) 1729
7. Benjamin Reichman and Allen J. Bard, *J. Electrochem. Soc.*, 12 (1979) 2133
8. A.P.Schuster, D.Nguyen and O.Caperilli, *Sol. Energy Mater. and Solar cells*, 13 (1986) 153
9. A.Scaffani, L.Palmisano, G.Marci and A.M.Venezia, *Sol. Energy Mater. and Solar Cells*, 51 (1998) 203
10. Toshiro Maruyama and Susumu Arai, *J. Electrochem. Soc.*, 141 (1994) 1021
11. Zhenuri Yu, Xiadong Fia, Zinhuri Du and Jiayen Zhang, *Sol. Energy Mater. and Solar Cells*, 64 (2000) 55
12. Micheal G.Hutchins, Nasser A.Kamel, Nabila EL.Kadry and Ahmed A.Ramaden, *Jpn. J. Appl. Physics*, 37 (1998) 4812
13. Kenchi Machido and Michio Enyo, *J. Electrochem. Soc.*, 137 (1990) 1169
14. P.R. Patil, *Mater. Chem. and Physics*, 69 (2001) 77
15. Nguyen Van Nha, Nguyen Thi Bao Ngoc and Nguyen Van Hung, *Thin Solid Films*, 334 (1998) 113
16. J.Arakaki, R.Reyes, M.Horn and W.Estrada, *Sol. Energy Mat. and Solar Cells*, 37 (1995) 33
17. Qiming Zhong Silvia, A.Wessel, B.Heinrich and Konard Colbow, *Sol. Energy Mat. Solar Cells*, 20 (1990) 289
18. Dae-Sik Lee, Ki-Hong Nam and Duk-Donog-Lee, *Thin Solid Films*, 375 (2000) 142
19. G.J.Fang, Z.L.Liu, G.C.Sun and K.L.Yao, *Phys. Stat. Sol. A.*, 43 (2001) 184
20. R.Vijayalakshmi, C.Sanjeeviraja and M.Jayachandran *Current Appl. Phys.*, 3 (2003) 171
21. R.Vijayalakshmi, C.Sanjeeviraja and M.Jayachandran *Proc. Solid State Ionics*, (2002) 445

22. R.Vijayalakshmi, C.Sanjeeviraja, M.Jayachandran and D.C.Trivedi, *Ionics*, 10 (2004) 151
23. R.Vijayalakshmi, C.Sanjeeviraja and M.Jayachandran, *Physics of Semiconductor Devices*, (IWPSD-2003), Narosa Publishing House, New Delhi (2004) 343
24. R.Vijayalakshmi, C.Sanjeeviraja and M.Jayachandran, (Communicated)
25. O.Bohnke and G.Robert, *Solid State Ionics*, 6 (1982) 115
26. M.S.Whittingham, *Solid State Ionic Devices*, Edited by B.V.RChowdri and S.Radhakrishnan (1988) 325-340
27. A.Magneli, *Acta.Shem.Scand.*, 7 (1953) 315
28. Chevrier, M.Touboul, A.Driouche and M.Figlarz, *J. Mater. Chem.*, 2 (1992) 639
29. A.Driouche, F.Abraham, M. Touboul and M.Figlarz, *Mater. Res. Bull.*, 26 (1991) 901
30. Oij A.Kishimoto and T.Kudo, *Nippon Kagaku Kaishi*, (1991) 1296-1301
31. Oij A.Kishimoto and T.Kudo, *J. Solid State Chem.*, 103 (1993) 176
32. Q.Zhong and K.Colbow, *Thin Solid Films*, 205 (1991) 85
33. A.Driouche, M.Figlarz and C.Delmas, *Solid State Ionics*, 62 (1993) 113
34. J.D.Guo, K.P.Reis and M.S.Whittingham, *Solid State Ionics*, 53-56 (1992) 305
35. L.Hernam, M.Macias, J.Morales, L.Sanchez and J.L.Tirado, *Solid State Ionics*, 48 (1991) 231
36. K.P.Reis, A.Ramanan and S.M.Whittingham, *J. Solid State Chem.*, 96 (1992) 31
37. P.Wiseman and P.G.Dickens, *J. Solid State Chem.*, 6 (1973) 374
38. R.Lechner, L.K.Thomas and Berlin, *Sol. Energy Mat. and Solar Cells*, 54 (1998) 139
39. Lianyuong Su, Lingang Zhang, Jinghu Fang and Nanjang, *Sol. Energy Mat. and Solar Cells*, 58 (1999) 133
40. P.M.S.Monk and S.L.Chester, *Electrochim. Acta*, 38 (1993) 1521
41. R.Hurditch, *J. Electronic. Lett.*, 11 (1975) 142
42. H.R.Zeller and H.U.Beyeler, *Appl. Phys.*, 13 (1977) 231
43. E.Kikuchi, Lida and A.Fujishima, *J. Electrochem. Soc.*, 351 (1993) 105
44. J.Zhang and K.Colbow, *J. Appl. Phys.*, 58 (1991) 1013
45. J.Zhang, S.A.Wessel and K.Colbow, *Thin Solid Films*, 185 (1990) 265
46. J.Zhaou, S.A.Wessel and K.Colbow, *J. Phys.D.*, 21 (1988) 1802
47. R.Sivakumar, A Moses Ezhil Raj, B.Subramanian, M.Jayachandran, D.C.Trivedi and C.Sanjeeviraja, *Mat. Res. Bull.*, 39 (2004) 1479
48. R.Sivakumar, M.Jayachandran and C.Sanjeeviraja, *Inorganic Materials: Recent Advances*, Narosa Publishing House, New Delhi (2004) 215
49. P.S.Patil, R.S.Patil and C.D.Lokande, *J. Pure and Applied Physics*, 35 (1993) 394
50. B.W.Faughnan and R.S.Cradall in display devices, edited by J.I.Pankove (Springer, Berlin, Heidelberg, 1980) Topics in *Appl. Phys.*, 140 181
51. R.Sivakumar, M.Jayachandran and C.Sanjeeviraja, *Mat. Chem. Phys.*, 87 (2004) 439
52. Takayo Kubo and Yoshinari Nishikitani, *Japan J. Electrochem. Soc.*, 145 (1998) 5
53. H.Kaneko, Nagao and K.Miyake, *J. Appl. Phys.*, 63 (1988) 510
54. H.M.Akram, Kitao and S.Yamada, *J. Appl. Phys.*, 63 (1989) 4364
55. D.Green, Properties of Tungsten oxide and tri gonally bonded compounds, Ph.D thesis, Univ of Sydney, Australia (1991)
56. B.F.Hichwa, G.Gaskey, D.F.Betz and J.D.Harlow, *J. Vac. Sci. Technol.*, A5 (1987) 1775
57. K.Kaneda and S.Suzuki, *Japan J. Appl. Phys.*, 30 (1991) 1841
58. N.A.Sesukin and A.A.Tsyganeko, *Zh. Fiz. Khim.*, 61 (1987) 159
59. H.Akram, Tatsuoka, M.Kitao and S.Yamada, *J. Appl. Phys.*, 62 (1987) 2030
60. L.E.Alexander, I.R.Beattie, A.Bukovszky, P.J.Jones, C.J.Marsden and G.J.Van Schalkwyk, *J. Chem. Soc. Dalton Trans.*, (1974) 81

61. C.J.Brinter, G.C.Frye, A.J.Hurd and C.S.Ashley, *Thin Solid Films*, 201 (1991) 97
62. C.J.Brinter, A.J.Hurd, P.R.Schunk, G.C.Frye and C.S.Ashley, *J. Non-Cryst. Solids.*, 121 (1990) 294
63. C.J.Brinter, A.J.Hurd, P.R.Schunk, G.C.Frye and C.S.Ashley, *J. Non-Cryst. Solids*, 147-148 (1992) 424
64. C.J.Brinter and G.W.Scherer, *Sol-Gel Science.*, (academic, Sandiego, 1990)
65. K.Hara, K.Kuoyama, H.Okabe, K.Matsushige and Y.Ishibashi., *J. Phys. Soc. Japan*, 61 (1992) 2147
66. J.Livage, M.Henry and C.Sanchez, *Prog. Solid State Chem.*, 18 (1988) 259
67. A.Chemseddine, *J. Non. Cryst. Solids.*, 147-148 (1992) 313
68. A.Chemseddine, F.Babonneau and J.Livage, *J. Non-Cryst. Solids*, 91 (1987) 271
69. A.Chemseddine, M.Henry and J.Livage, *Rev.Chim. Minerale*, 21 (1984) 487
70. A.Chemseddine, R.Morineau and J.Livage, *Solid State Ionics*, 9-10 (1983) 357
71. A.Chemseddine, R.Morineau and J.Livage, *Vide Couches Minces.*, 222 (1984) 239.
72. M.A.Habib, *Proc. Soc. Photo-Opt, Instrum.Engr.*, 1149 (1989) 46
73. M.Habib and D.Glueck, *Sol. Energy Mat. and Solar Cells*, 18 (1989) 127
74. P.Judeinstein and J.Livage, *Mater. Sci. Engr.*, B3 (1989) 129
75. P.Judeinstein, and J.Livage, *Proc. Soc. Photo-Opt. Instr. Engr.*, 328 (1990) 344
76. T.Minami, H.Sato, H.Nanto and S.Takata, *Thin Solid Films*, 176 (1989) 277
77. T.Nanba, Y.Nishiyama and I.Yasui, *J. Mater. Res.*, 6 (1991) 1324
78. Kil Don Lee, *Sol. Energy Mat. and Solar Cells*, 57 (1999) 21
79. J.M.Bell, D.C.Green, A.Patterson, G.B.Smith, K.A.MacDonald, K.Lee, J.D.Kirkup, B.O.Cullen, I.West, Spiccia, M.J.Kenny and L.Swielunski, *Proc. Soc. Photo-opt Instrum. Eng.*, 1536 (1991) 29
80. Toshiro Maruyama and Susumu Arai, *J. Electrochem. Soc.*, 141 (1994) 021
81. P.K.Shen, A.C.Tesung, *J. Mater. Chem.*, 2 (1992) 1141
82. Su Lianyong, Wangl., Hang. Lu and Zuhong, *Mater. Chem. Phys.*, 56 (1998) 266
83. D.Green, J.MBell and G.B.Smith, *Proc. Soc. Photo-opt Instrum. Engg.*, 25 (1986) 1420
84. B.Orel, Uopera Krasovec and Lavrensic Stanger, *J. Solgel. Sci. Tech.*, 11 (1998) 87
85. B.Orel, U.Opera Krasovec, M.Macek, F.Svegl. U Larvensic Stager, *Sol. Energy. Mat. and Solar Cells.*, 56 (1999) 343
86. Nobuyuki Yoshiike, Masatake Ayusawa and Siego Konda, *J. Electrochem. Soc.*, 131 (1984) 2600
87. Nobuyuki Yoshiike, Yosuo Mizuno and Siego Konda, *J. Electrochem. Soc.*, 131 (1985) 2634
88. Nobuyuki Yoshiike, Yosuo Mizuno and Siego Konda, *J. Electrochem. Soc.*, 130 (1983) 2283
89. Eianyong Su, Lingang Zhang, Jihguai Pang, Minhua Xu, Zuhong Lu, *Sol. Energy Mat. and Solar Cells*, 58 (1999) 133.
90. T.Ohtsuka, Noboru Goto and Nairo Sato, *J. Electroanal. Chem.*, 287 (1990) 249
91. Nobuyuki Yoshiike, Yosuo Mizuno and Siego Konda, *J. Electrochem. Soc.*, 131 (1985) 2634
92. P.Judeinstein and J. Livage, *Proc. SPIE.*, 1328 (1990) 344.
93. Nilgun Ozer, Carl. Lampert, *Sol. Energy Mat. and Solar Cells*, 54 (1998) 147
94. A.Chemseddine, R.Morineau and J.Livage, *Solid State Ionics*, 27 (1998) 19
95. H.Unuma, K.Tanooka Y.Suzuki, T.Farasaki, K.Kodira and T. Matsushita, *J. Mater. Sci. Letters*, 5 (1986) 1248
96. A.M.Habib and D.Glueck, *Sol. Energy. Mat. and Solar Cells*, 18 (1989) 127
97. R.Lechner and L.K.Thomas, *Sol. Energy Mat. and Solar Cells*, 54 (1998) 139
98. A.Guerfi, W. Paynter and L.Dao, *J. Electrochem. Soc.*, 142 (1995) 1469

99. P.Judeinstein, A.Chemseddine and C.Sanchez, *J. Chim. Phys.*, 89 (1992) 1469
100. P.Judeinstein and J.Livage, *J. Mater.Chem.*, 1 (1991) 621
101. P.Judeinstein and J.Livage, *J. Chim. Phys.*, 90 (1993) 1137
102. P.Judeinstein, R.Morineau and J.Livage, *Solid State Ionics*, 51 (1992) 239
103. T.Nanba and I.Yasui, *J. Solid State. Chem.*, 83 (1989) 304
104. K.Nonaka, A.Takase and K.Miyakawa, *J. Mater. Sci. Lett.*, 12 (1993) 274
105. K.H.Tytko and O.Glemser, *Advances in Inorganic Chemistry and Radiochemistry*, edited by H.J.Emeelus and A.G.Sharpe; 19 (1999) 239
106. H.Akram, M.Kitao and S.Yamada, *J. Appl. Phys.*, 66 (1989) 4364
107. M.F.Daniel, B.Desbat, J.C.Lassegues and R.Garie, *J. Solid. State. Chem.*, 73 (1988) 127
108. L.Pickleman and P.Schlotter, in *Proc, First European Display research Conf., Eurodisplay' 81* (Munche. Sept., 1981)
109. S.Badilescu, P.V.Ashrit, F.E.Girouard and Vo-van Truong, *J. Electrochem. Soc.*, 136 (1989) 3599
110. S.Yamada, S.Yoshida and M.Kitao, *Solid State Ionics*, 40-41 (1990) 487
111. S.K.Deb, *Philos. Mag.*, 27 (1973) 801
112. S.K.Deb, in *Proc.24<sup>th</sup> Electronic Component Conf. (IEEE)*, Washington, (1974) 11
113. M.Green, H.I.Evan and Z.Hussain, in *second Int. Sym. Polymer electrolytes*, edited B.Scrosati, Elsevier Appl. Sci., London (1990) 449
114. M.Green and Z.Hussain, *J. Appl. Phys.*, 69 (1991) 7788.
115. M.Green and A.Travlos, *Philos. Mag.*, B 51 (1984) 501
116. H.K.Kaneko, Miyake and Y. Termato, *J. Appl. Phys.*, 53 (1982) 3070.
117. Miyake H Kaneko, M.Sano, N.Suedomi, *J. Appl. Phys.*, 55 (1984) 2747
118. A.Nakamura, T.Kawauchi, K.Urabe, M.Kitao and S.Yamada, *J. Vac. Soc. Japan*, 24 (1981) 471
119. M.Sharon, M K Sharan and SR.Jawalikar, *Sol. Energy Mat. Solar Cells*, 10 (1984) 329
120. A.M.Soloduha and O.K.Zhukov Izy Akad. Nauk. USSR. *Neorg. Mater.* 26 (1990) 2335. [published in *Inorgan.Mat* 26, 2002-2004 (1990)]
121. Yoshimura M.Watenbe, Y.Koike K.Kiyota and M.Tnaka, *J. Appl. Phys.*, 53 (1982) 7314
122. Miyake H Kaneko, M. Sano and N.Suedomi, *J. Appl. Phys.*, 55 (1984) 2747
123. B.W.Faughman, R.S.Crandall and P.M.Hayman, *RCA, Rev.*, 36 (1975) 177
124. M.Green and A.Travlos *Philos, Mag.B.*, 51 (1984) 501
125. M.Kitao, S.Yamada, S.Yoshida, H.Akram and K.Urabe, *Sol. Energy Mat. Solar Cells*, 25 (1992) 241
126. K.Miyake, H.Kaneko Suedomi and S.Nishimoto, *J. Appl. Phys.*, 54 (1983) 5256
127. Akram Tatsuka, M.Kitao and S.Yamada, *J. Appl. Phys.*, 62 (1987) 2039.
128. Kaneko HK.Miyake, Y.Termato, *J. Appl. Phys.*, 53 (1982) 3070
129. H.Kaneko, Nagao and K.Miyake, *J. Appl. Phys.*, 63 (1988) 510
130. M.Kitao, S.Yamada, S.Yoshida, H.Akram, K.Urabe *Sol. Energy Mat. Solar Cells*, 25 (1992) 41
131. H.Akram, M.Kitao and S.Yamada, *J. Appl. Phys.*, 66 (1989) 4364
132. M.Kitao, S.Yamada, S.Yoshida, H.Akram and K.Urabe *Sol. Energy Mat. Solar Cells.*, 25 (1992) 241
133. D.Davazoglou, G.Leveque and A.Donnadieu, *Sol. Energy Mat. Solar Cells.*, 17 (1988) 379
134. A.Donnadieu, D.Davazoglou and A.Abdellaoui, *Thin Solid Films*, 164 (1988) 333
135. Delichere P.P.Falaras and A Hugot-LeGoff, *Proc. Soc. Phot-Opt Instrum. Engg.*, 1016 (1988) 12
136. Delichere P.P.Falaras and AHugot-LeGoff, *Thin Solid Films*, 161 (1988) 47
137. Delichere P.P.Falaras, AHugot-LeGoff and N.Yu, *J. Electrochem. Soc.*, 133 (1986) 2106
138. F.Di Quarto, A.DiPaola, S.Piazza and C.Sunseri, *Sol. Energy Mat.: Solar Cells*, 11 (1985) 419

139. F.Di Quarto, G Russo, *J. Chem. Soc. Faraday. Trans.*, 178 (1982) 3433
140. F.Di Quarto, A.Di Paola and C.Sunseri, *Electrochim. Acta*, 26 (1981) 1177
141. D.V.Sviridov and A.IKulak, *Thin Solid Films*, 198 (1991) 191
142. F.P.Koffberg, K.Dwight and A.Wold, *Solid State Commun.*, 30 (1979) 433
143. Takaya Kubo and Yoshinori Nishikitani, *J. Electrochem. Soc.*, 145 (1998) 1729
144. Green and M.Hussain, *J. Appl. Phys.*, 69 (1991) 7788
145. Nakumura.AT.Kawauchi, K.Urabe, M.Kitao and S.Yamada, *J. Vac. Soc. Japan*, 24 (1981) 471
146. K.Von Rottkay, N.Ozer, M.Rubin and T.Richardson *Thin Solid Films*, 308 (1997) 50
147. R.Ramachandran, Pradeep and S.A.Agnihotry, *Indian J. Pure and Applied Physics*, 137 (1999) 353
148. A.Temmink, O. Anderson, K.Bange, H.Hantsche and Yu, *Vacuum*, 41 (1990) 1144
149. A.Azens, A.Hjelm, D.LeBellac, C.G.Granqvist., J.Berczynska, E.Pentjuss, J.Gabrusenoks and J.M.Wills, *Solid State Ionics*, 86 (1996) 943
150. S.F.Cogen, T.D.Planante, M.A.Parker, *J. Appl. Phys.*, 60 (1986) 2735
151. F.O.Arntz and R.B.Golder, *J. Appl. Phys.*, 67 (1990) 3177
152. S.G.Golden and B.H.Steele, *Solid State Ionics*, 28-30 (1987) 1733
153. G.Bader, P.V.Ashrit and Vo-Van Truong, *Appl. Optics*, 37 (1998) 1146
154. Micheal G.Hutchins and Nasser A.Kamel, *Jpn. J. Appl. Phy.*, 17 (1998) 4812
155. P.V.Ashrit, G.Bader and Vo-van Truong, *Thin Solid Films*, 320 (1998) 324
156. Micheal G Hutchins and Nasser A. Kamel, *Jpn. J. Appl. Phy.*, 17 (1998) 4812
157. F.Micalak and P.Alderbert, *Solid State Ionics*, 87 (1996) 265
158. B.Orel, N.Groselj, U.Opara Krasovec, M.Gabrscek, P.Bukovec and R.Reisfeld, *Sensors and Actuators B.*, 50 (1998) 234
159. E. Pascual, J.Marti., E.Garcia, A.Canillas and E.Bertran, *Thin Solid Films*, 313 (1998) 682
160. P.M.S.Monk, J. Mortimer and D.R.Rosseinsky, *Electrochromism: Fundamental and applications*, VCH Weinheim, (1995)